IEEE Transactions on Quantum Engineering

Received 5 September 2023; revised 13 November 2023; accepted 28 November 2023; date of publication 4 December 2023; date of current version 2 January 2024.

Digital Object Identifier 10.1109/TQE.2023.3338970

Exploiting the Quantum Advantage for Satellite Image Processing: Review and Assessment

SORONZONBOLD OTGONBAATAR[1,2] AND DIETER KRANZLMÜLLER[2]

[1]Remote Sensing Technology Institute, German Aerospace Center DLR, 82234 Weßling, Germany
[2]Institut für Informatik, Ludwig-Maximilians-Universität München, 80538 München, Germany

Corresponding author: Soronzonbold Otgonbaatar (e-mail: soronzonbold.otgonbaatar@dlr.de).

This work was supported by the European Space Agency through Project Quantum Advantage for Earth Observation (QA4EO).

ABSTRACT This article examines the current status of quantum computing (QC) in Earth observation and satellite imagery. We analyze the potential limitations and applications of quantum learning models when dealing with satellite data, considering the persistent challenges of profiting from quantum advantage and finding the optimal sharing between high-performance computing (HPC) and QC. We then assess some parameterized quantum circuit models transpiled into a Clifford+T universal gate set. The T-gates shed light on the quantum resources required to deploy quantum models, either on an HPC system or several QC systems. In particular, if the T-gates cannot be simulated efficiently on an HPC system, we can apply a quantum computer and its computational power over conventional techniques. Our quantum resource estimation showed that quantum machine learning (QML) models, with a sufficient number of T-gates, provide the quantum advantage if and only if they generalize on unseen data points better than their classical counterparts deployed on the HPC system and they break the symmetry in their weights at each learning iteration like in conventional deep neural networks. We also estimated the quantum resources required for some QML models as an initial innovation. Lastly, we defined the optimal sharing between an HPC+QC system for executing QML models for hyperspectral satellite images. These are a unique dataset compared with other satellite images since they have a limited number of input quantum bits and a small number of labeled benchmark images, making them less challenging to deploy on quantum computers.

INDEX TERMS Earth observation (EO), hyperspectral images, image classification, quantum computers, quantum machine learning (QML), quantum resource estimation, remote sensing.

I. INTRODUCTION

A. WHY QUANTUM COMPUTING FOR EARTH OBSERVATION?

Earth observation (EO) methodologies tackle optimization and artificial intelligence (AI) problems involving big datasets obtained from instruments mounted on spaceborne and airborne platforms. Some optimization and AI problems combined with big EO datasets are intractable computational problems for conventional high-performance computing (HPC) systems. In addition, EO datasets themselves are complex heterogeneous image datasets, compared with conventional red-green-blue images, characterized by so-called 4 V features comprising *volume*, *variety*, *velocity*, and *veracity* [1]; here, *volume* refers to big EO datasets (e.g., terabytes of data per day collected, for instance, by the European Space Agency); *variety* refers to distinct spectral data, such as multispectral and hyperspectral pixel data; *velocity* refers to the speed of change on the Earth's surface; and *veracity* refers to imperfect datasets, such as noisy images or remotely sensed images, partly covered by clouds [2]. In general, EO problems also include calibration and integer optimization problems in synthetic aperture radar applications [3], [4], a Bayesian paradigm (e.g., Gaussian processes) for retrieving physical parameters from remotely sensed datasets [5], [6], uncertainty estimates for EO predictions [7], solving partial differential equations (PDEs) for climate modeling and digital twin Earth paradigms [8], and identifying objects on the Earth's surface [9]. Furthermore, some computational problems like AI training architectures are computationally expensive and inherently intractable problems or NP-hard problems (see Fig. 1) [10]; nondeterministic (NP) polynomial problems are computational problems where there

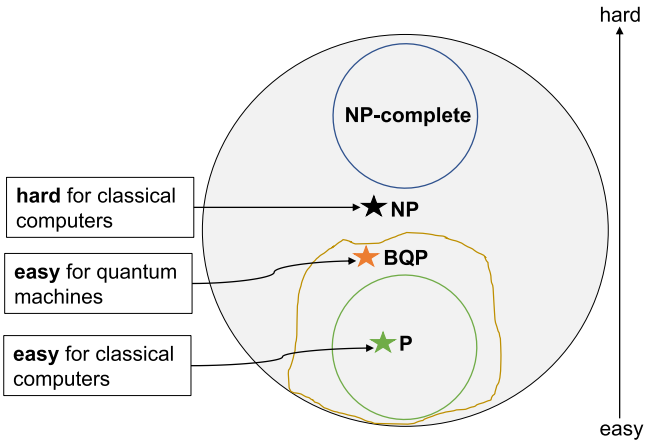

FIGURE 1. Computational complexity conjecture draws boundaries between computational problems according to their hardness based on the required classical and quantum computational resources. In particular, the computational problem denoted by the green star is easy to solve for both quantum machines and classical computers, the computational problem denoted by the orange star is easy for quantum machines but hard for classical machines, and the computational problem denoted by the black star is hard for classical computers. Still, no known efficient quantum algorithmic approaches exist for quantum machines.

are no known efficient commonly used algorithms for finding their solutions in a reasonable polynomial time (i.e., a polynomial number of steps) but can be verified in a polynomial time given their solutions, and NP-hard problems are computational problems harder than NP problems. On the other hand, quantum machines harnessing quantum physics phenomena like entanglement can solve some challenging problems faster and more efficiently than their counterpart conventional machines ranging from integer optimization problems [11], [12], [13] to AI techniques [14], [15], [16], [17], [18], and PDEs, [19], [20], and even quantum-inspired algorithms for solving PDEs [21]. Thus, quantum algorithms' computational advantages (or quantum advantage) over conventional algorithms inspire enough to examine and identify computationally intractable problems with EO methodologies and hard EO datasets for near- and far-term quantum machines. We note that the terms "quantum machine" and "quantum computer" are generally interchangeable. However, the former is used to describe current quantum platforms that operate at a hardware level, rather than at the level of a classical computer.

B. DO WE REALLY NEED QUANTUM MACHINES?

Quantum machines can be generally divided into three families comprising quantum annealers [22], quantum simulators [23], [24], and universal quantum computers [25]. These quantum machines promise computational advantage for computing notoriously difficult problems over conventional computers according to computational complexity theorems/conjectures [26], [27]; computational complexity theorems draw boundaries between computational problems according to their hardness for finding their solutions (see Fig. 1) [10]. At the moment, quantum machines are designed to tackle specific forms and kinds of intractable computational problems, e.g., quantum annealers for quadratic unconstrained binary optimization (QUBO) problems or simulating the Ising Hamiltonian [11], and quantum simulators for mimicking some physical Hamiltonian [28], [29]. Research communities ranging from high-energy physics [24], condensed-matter physics [29], AI [15], to EO [30] are in the exploration phase of identifying and investigating their hard problems for quantum platforms. Furthermore, classical computational methods for intractable computational problems reach their limitations and potential accuracy due to the classical computational resource required and the complexity of both EO challenges and datasets. As stated earlier, some computational techniques are intractable problems on conventional machines and computationally expensive, even on the HPC system. Thus, to go beyond current computational methods integrated with large-scale datasets to find a better solution and utilize low computational cost, it is inevitable to examine and identify computationally demanding problems in EO applications for novel near- and long-term quantum machines. More importantly, gaining insight into programming these novel computing machines and their potential advantages and imperfections for computational problems is vital.

C. STATE OF THE ART OF QC FOR EO

Quantum computing (QC) is a novel computing paradigm that promises to find solutions to some intractable computational problems more efficiently and faster by exploiting quantum superposition and entanglement than conventional computing techniques if and only if one considers ideal quantum complexity measures without overhead considerations like a distillation of Toffoli gates in the real quantum machines, e.g., the classical versions of the Toffoli gates are transistors in a conventional computer [31]. Quantum machines are a kind of computer constructed using the primitives of a QC method, such as quantum bits (qubits) and quantum gates, in contrast to traditional classical bits and transistors. Digital quantum machines can be decomposed into the following three layers [32]:

1) a *quantum state preparation* or a *quantum data encoding* layer;
2) a *quantum unitary evolution* or a *parametrized quantum gate* layer;
3) a *quantum measurement* layer.

For gaining insight into computing EO problems involving big datasets on quantum machines, some studies already exist for processing a *variety* of EO datasets to tackle EO challenges using hybrid classical–quantum approaches (see Fig. 2). Hybrid classical-quantum approaches involve the use of a classical computer to enhance quantum algorithms. Quantum machine learning (QML) is a type of hybrid classical-quantum approach, which is interchangeable with quantum artificial intelligence. It is also worth noting that a

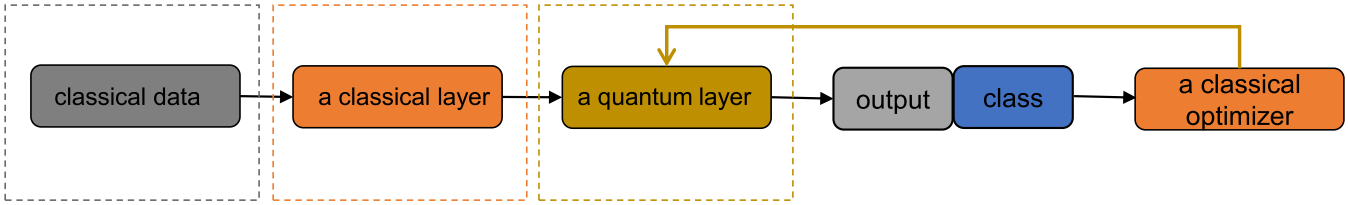

FIGURE 2. Hybrid classical-quantum approach for computational and machine learning tasks. A quantum layer includes implicitly quantum data encoding, parametrized quantum gates, and quantum measurement layers.

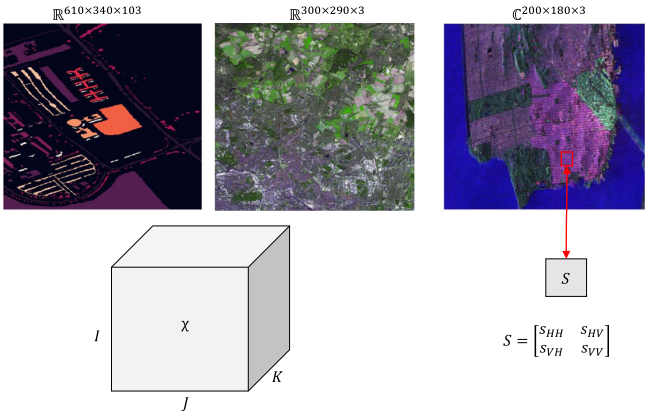

FIGURE 3. (Top) Example hyperspectral, multispectral, and polarimetric images, (bottom Left) their third-order tensor representation, and (bottom right) each pixel/target in polarimetric images is characterized by the complex numbered scattering matrix in contrast to hyperspectral and multispectral images. Here, s_{ij} denotes a scattering element given sent/reflected horizontal *H* or vertical *V* polarized beam.

variety of datasets includes hyperspectral, multispectral, and polarimetric EO images.

1) EO IMAGES

We can generalize that EO images are third-order tensors regardless of a *variety*. Furthermore, a hyperspectral image is a remotely sensed image denoted by $\mathbb{R}^{I\times J\times K}$, where I and J are its spatial dimensionality, and K means hundreds of its narrow-spaced spectral bands (or features), e.g., the Pavia University, hyperspectral image described by $\mathbb{R}^{610\times340\times103}$ tensor. Multispectral images are a third-order tensor $\mathbb{R}^{I\times J\times K}$ with at most $K = 12$ spectral bands. The main difference between them is the spectral bands' number and spacing. In contrast, polarimetric images are characterized by the scattering property S of ground targets; each pixel is described by a 2×2 scattering matrix but not by spectral bands as in hyperspectral and multispectral images. Hence, we could assume that polarimetric images have $K = 3$ informative features if the scattering matrix is symmetric and $K = 4$ informative features otherwise (see Fig. 3) [33].

2) QML FOR EO IMAGES

Climate AI tasks involve analyzing satellite images that consist of thousands of pixels and hundreds of spectral bands. For example, Eurosat multispectral images have a size of 64×64 pixels and 12 spectral bands, which can be represented as $\mathbb{R}^{64\times64\times12}$ [34]. In contrast, the digital quantum machines currently available on the market have less than a hundred noisy qubits and around depth-five of faulty quantum gates [35]. Therefore, the main challenge is to embed satellite images in a *quantum data encoding* layer, regardless of the size of quantum machines and their quantum errors. To address this challenge, the authors in [36] and [37] proposed and utilized a two-level embedding scheme. This scheme comprises a classical layer for dimensionality reduction and a *quantum data encoding* layer for dimensionally reduced images. In other words, they used a hybrid classical-quantum approach, embedding classical datasets in a *quantum data encoding* layer and optimizing a *parametrized quantum gate* layer of digital quantum computers with the help of a conventional classical computer. However, the Eurosat dataset they used is a large dataset consisting of low-dimensional and easy-to-classify images and thus has low *veracity*. Most EO datasets, on the other hand, are small datasets containing high-dimensional and hard-to-classify images or high *veracity* images. For example, the multispectral UC Merced Land Use dataset has a size of 245×245 pixels and three spectral bands, which can be represented as $\mathbb{R}^{245\times245\times3}$ [38]. To investigate the performance of quantum machines with varying depths of a *parametrized quantum gate* layer, Otgonbaatar et al. [39] utilized this dataset and polarimetric EO images for natural embedding in input qubits without a dimensionality reduction technique [40]. It is important to note that the quality of the datasets used plays a crucial role in data-driven tasks for hybrid classical-quantum approaches [41]. Therefore, Gupta et al. [42] analyzed the power of EO image datasets for training digital quantum machines.

Furthermore, a quantum annealer is a type of quantum simulator that is designed to simulate an Ising Hamiltonian equivalent to QUBO problems [22]. The authors in [43], [44] analyzed classification problems posed as QUBO problems, belonging to NP-hard problems, on a D-Wave quantum annealer. They employed binary hyperspectral EO images since a D-Wave quantum annealer promises to converge to a better solution to NP-hard problems. Some studies also transformed a support vector machine (SVM) into a QUBO problem [45] and optimized it on a D-Wave quantum annealer when analyzing EO image datasets [33], [46]. To embed large EO datasets in a D-Wave quantum annealer, Otgonbaatar et al. [47] used a K-fold technique and the concept of a coreset since a D-Wave quantum annealer has around

5000 qubits arranged according to an expressly limited topology. A D-Wave quantum annealer was also proposed for a notoriously hard feature selection task and multilabel SVM for remotely sensed hyperspectral images [48].

Lastly, quantum-inspired algorithms are becoming increasingly popular in both academic and industrial circles due to their energy and computational efficiency. These algorithms are inspired by the potential advantages of quantum algorithms, such as the quantum-inspired quantum Fourier transformation [49], quantum-inspired AI/ML [50], and the use of tensor networks to compress deep neural networks [51]. Tensor networks are designed to compute quantum many-body systems efficiently [52], and they are currently being used to simulate quantum circuits on modern GPU tensor cores [53]. Thanks to these advancements, quantum tensor networks have been successfully utilized to decrease the weights of physics-informed neural networks and increase the resolution of hyperspectral images [54].

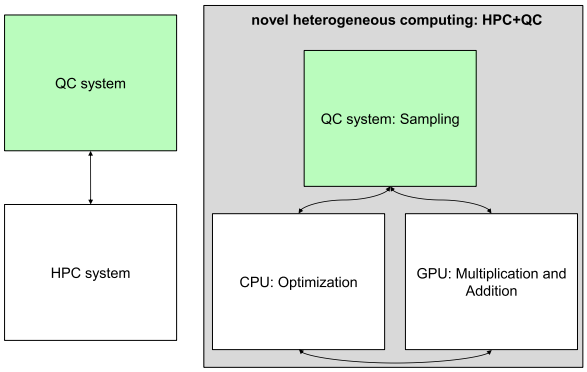

FIGURE 4. Novel heterogeneous computing. A high-performance and QC paradigm. Here, conventional heterogeneous computing refers to the programming of CPU and GPU, whereas we call novel heterogeneous computing when integrating QPUs with CPUs and GPUs. QPUs can be several parallel quantum machines based on different quantum technologies such as quantum annealing, neutral atoms, superconducting, and photonic.

3) SELECTING EO DATA FOR QUANTUM MACHINES

When working with quantum machines in EO challenges, it is vital to choose remotely sensed datasets based on the principle that "the more features in the dataset, the less quantum resources required." Studies have shown that processing multispectral images requires more quantum gates and qubits than hyperspectral and polarimetric images [36], [40]. This is because multispectral images need global feature capturing, with each pixel dependent on its neighbors, making processing more resource-intensive. On the other hand, hyperspectral and polarimetric images contain informative spectral information for each pixel. They can be embedded in qubits without the constraint of their neighbors, making processing less resource-intensive [40]. For instance, one QML model known as a quantum convolutional neural network (QCNN) requires approximately 4000 quantum gates only to embed the element $\mathbb{R}^{64\times64\times12}$ in the Eurosat dataset and roughly 60 000 quantum gates for embedding the multispectral image $\mathbb{R}^{300\times290\times3}$ illustrated in Fig. 3 in the input qubits [55]. Hence, multispectral images are not viable for deploying QCNNs on today's quantum machines, even on future quantum machines. However, a hybrid classical-quantum model requires fewer quantum resources than QCNNs. Otgonbaatar and Datcu [36] used only 16 quantum gates for encoding the Eurosat and the multispectral image $\mathbb{R}^{300\times290\times3}$ depending on the compressing quality. In contrast, we can embed the pixels of a hyperspectral image, e.g., the Pavia University hyperspectral image, in the input qubits using only at least three and, at most, about 103 quantum gates thanks to their abundant spectral bands [33]. As for polarimetric images, we need at most five quantum gates due to their doppelgänger feature to qubits or the one-to-one mapping between polarimetric images and qubits [40].

Based on the above analysis, hyperspectral satellite images are much more appropriate for designing and assessing QML models and tackling climate challenges than multispectral and polarimetric images since they have abundant spectral information and fewer quantum resources required than other remotely sensed datasets. More importantly, QML models generalize better on small-scale datasets than their classical alternatives [56], whereas a hyperspectral dataset has limited labeled images (or small-scale datasets) compared to multispectral datasets and has more features than both multispectral and polarimetric datasets.

D. HOW AND WHEN DO QUANTUM MACHINES OUTPERFORM CONVENTIONAL COMPUTERS?

It is becoming increasingly clear that quantum processing units (QPUs) will soon be working alongside conventional classical computers, such as how central processing units (CPUs) and graphics processing units (GPUs), are used in heterogeneous computing [30]. We are currently in the era of HPC, and the emergence of QC is a new and exciting concept in heterogeneous computing. It involves integrating a CPU+GPU with QPUs designed to handle specific computational problems (see Fig. 4). For instance, a quantum annealer is designed to tackle only QUBO problems, and neutral atom platforms can simulate certain chemical Hamiltonians. Depending on the difficulty level of the computational problems, we may need to program a challenging heterogeneous computing environment (i.e., CPU+GPU+QPUs) or a conventional one (i.e., CPU+GPU).

QPUs, except for quantum annealers, currently consist of around 100 error-prone qubits and low-depth, faulty quantum gates. Preskill [57] coined these devices as "noisy intermediate-scale quantum (NISQ) devices." However, for practical computational problems, there is no demonstration of the computational advantage of NISQ devices over a conventional classical computer. Therefore, estimating the quantum resources required to tackle hard computational and ML problems is vital to achieving a quantum advantage in EO. It is worth noting that some quantum algorithms can be simulated efficiently using a conventional classical computer. For

this reason, any reasonable quantum resource estimation of a quantum algorithm should consider non-Clifford T-gates, error rates of qubits and quantum gates, and the execution time of single- and two-qubit quantum gates [58].

Non-Clifford T-gates are the most resource-expensive part of implementing a quantum algorithm, compared with Clifford quantum gates or CNOT, Hadamard, Phase, and measurement gates. Even the Gottesman–Knill theorem states (informally) that non-Clifford T-gates cannot be efficiently simulated on a conventional classical computer. In contrast, Clifford quantum gates can be simulated in polynomial time using a conventional classical computer without any restriction on entanglement [58], [59]. Specifically, quantum algorithms consisting only of Clifford quantum gates can be simulated in $\mathcal{O}(n^2 m)$ polynomial steps with n qubits and m Clifford operations. However, quantum algorithms consisting of Clifford+T gates take exponential steps $\mathcal{O}(\kappa t^3 \epsilon^{-2})$, with the number of T-gates known as T count (t), stabilizer state (k) growing exponentially $\mathcal{O}(2^t)$, and an error rate (ϵ) [58]. We note that some quantum algorithms can be efficiently simulated using a sophisticated classical technique like a tensor network on GPU tensor cores [60].

The Clifford+T gate set $\{S, H, \text{CNOT}, T\}$ is considered a universal gate set for digital QPUs. This is due to the feasibility of quantum error-correcting, known as a surface code [61]. More importantly, the surface code enables the creation of fault-tolerant digital quantum computers that surpass the NISQ-era computers [35]. In contrast to NISQ computers, fault-tolerant quantum computers are made up of error-free qubits and quantum gates that are transpiled into the Clifford+T gate set. Therefore, this shows that for quantum advantage in EO applications to be reached if and only if our quantum learning models have a sufficiently high number $\mathcal{O}(10^{12})$ of T-gates and generalize on unseen data points [62]. Otherwise, we can simulate them efficiently using conventional classical computing resources.

Further, a hybrid classical-quantum approach for computational EO problems is embedding high-dimensional classical data in a limited number of qubits and optimizing the weights of a parameterized quantum model [36], [63]. There is yet another challenging question: how notoriously difficult computational problems can take advantage of both HPC and QC systems or when we should execute them on an HPC instead of a QC system and vice versa. We decompose the parameterized quantum model into the Clifford+T gate set at each learning iteration to tackle these issues. If the parameterized quantum model only includes Clifford gates and a small number of T-gates [64], then we execute it on the HPC system instead of the QC machines since we already know that Clifford gates and hundreds of T-gates can be simulated efficiently using a conventional classical computer. We re-emphasize that quantum learning models can be simulated efficiently using a classical computer without the need for quantum computers if they do not have a high number of T-gates.

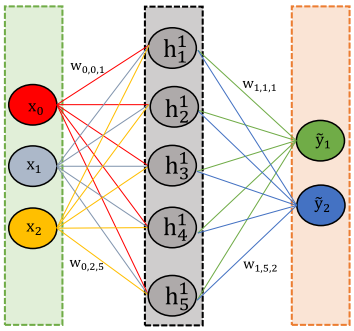

FIGURE 5. Visual representation of traditional neural networks.

1) QML—SYMMETRY-BREAKING

Symmetry-breaking refers to asymmetric tunable weights of traditional ML models such that the weights capture and rank the dataset's features during training. Consider a neural network with a single hidden layer illustrated in Fig. 5. Mathematically, it is defined

$$h_i^1 = f\left(w_{0,i} + \sum_{j=0}^{2} w_{0,j,i} x_j\right), \quad i = 1, \ldots, 5 \tag{1}$$

$$\tilde{y}_l = f\left(h_{0,l} + \sum_{j=1}^{5} w_{1,j,l} h_j^1\right), \quad l = 1, 2 \tag{2}$$

where $f(\cdot)$ is a nonlinear activation function, w's denotes a tuneable weight, and x_k is the dataset's feature. We note that w's must have different values identical to a linear regression model $\tilde{y} \sim w_0 + w_1 \cdot x_0 + w_2 \cdot x_1$. If the model weights are symmetric $w_1 = w_2$, it has not learned the dataset's feature. To capture the dataset's feature, the learning model must have asymmetric weights $w_1 \neq w_2$, or the learning model must break the symmetry in its weights. Identical to the symmetry-breaking in conventional ML, Haug et al. [18] implicitly demonstrated that QML models also must break symmetry in their weights, resulting in better generalizability or more expressive power and higher effective dimension than their classical counterparts. In particular, they identified and disregarded some redundant weights in their quantum models that are symmetric (e.g., the same digital values) and do not simultaneously increase the QML model's expressive power. They, however, did not estimate the hardness of their QML models characterized by non-Clifford T-gates that can be implemented efficiently on quantum machines and otherwise difficult on conventional HPC systems.

Furthermore, to outperform classical learning models deployed on an HPC system, we should invent and design QML models having thousands of T-gates, and their expressive power (signaling the symmetry-breaking in QML models) is higher than their classical counterparts [16]. There is (still) no such QML model with thousands of T-gates and higher expressive power on unseen data points than its classical counterpart.

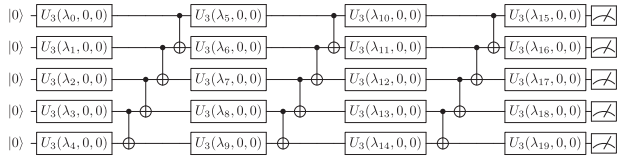

FIGURE 6. We transpiled a real-amplitude quantum circuit having depth-one into the Clifford+T and the native gate set. It is used to demonstrate the power of a PQC model by Abbas et al. [16].

II. QUANTUM RESOURCE ESTIMATION FOR HYPERSPECTRAL IMAGES

A hyperspectral imaging satellite, such as the EnMAP satellite,[1] is a type of imaging instrument mounted on a satellite and used to sense spectral reflectances. The mission of this satellite is to collect hyperspectral imaging data that provides crucial information for scientific inquiries, societal grand challenges, and key stakeholders and decision-makers. This information pertains to various topics, such as climate change impact and interventions, hazard and risk assessment, biodiversity and ecosystem processes, land cover changes, and surface processes.

We already have seen that hyperspectral images require less quantum resources than other remotely sensed datasets. They also have limited label information, and there is limited availability of benchmark hyperspectral images compared with conventional benchmark remote-sensing datasets, such as multispectral images [65], [66]. When training QML models on limited benchmark-oriented labeled hyperspectral image datasets, a classical layer can reduce the dimensionality of the hyperspectral image dataset's spectral bands due to the limited number of input qubits. However, the degree of dimensionality reduction required for the given hyperspectral image dataset depends on the utilized quantum machines. Regardless of their error, this means whether we can access a quantum machine with qubits ≤ 100 or > 100. The role of classical machines in preprocessing the hyperspectral image dataset is reduced as we can feed many informative features to a quantum machine with less dimensionality reduction, especially as the number of qubits of quantum machines increases. We assume we used EnMAP hyperspectral images with 103 spectral bands and 610×340 spatial dimensions. The EnMAP hyperspectral images also have 207 400 data points and 103 features, which are small-scale image datasets compared with conventional multispectral images. To execute the QML model on the quantum machine having $\leq$100 input qubits, we can either reduce the spectral bands of the EnMAP hyperspectral images from 103 to at most 100 or select the most informative 100 bands to be compatible with the input qubits by utilizing a classical machine. Instead, for quantum machines with more than 100 input qubits, we can use a classical machine to persevere more spectral bands of the EnMAP hyperspectral images when performing the dimensionality reduction or the feature selection technique in the spectral bands.

[1] https://www.enmap.org/mission/

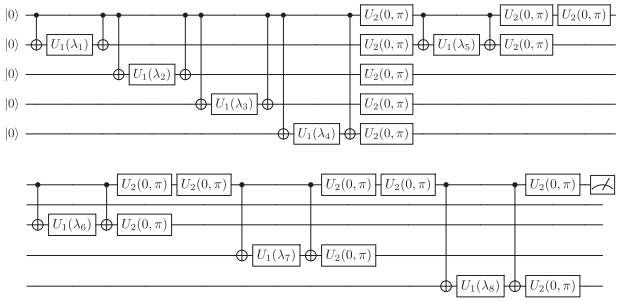

FIGURE 7. We transpiled an energy-based quantum circuit having depth-one into the Clifford+T and the native gate set. This PQC model is proposed for the NISQ device by Farhi and Neven [68].

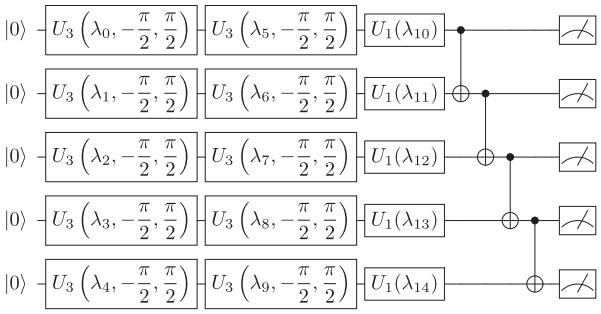

FIGURE 8. We transpiled a strongly entangling quantum circuit having depth-one transpiled into the Clifford+T and the native gate set. This PQC model is proposed to build a powerful quantum learning model by Schuld et al. [73].

Toward quantum resource estimation, we assessed four different PQC models expressed by the Clifford+T gate set (see Figs. 6–9). The Clifford+T gate set is defined by U_1, U_2, U_3, and CNOT gates

$$U_1(\lambda) = \begin{pmatrix} 1 & 0 \\ 0 & e^{i\lambda} \end{pmatrix} \quad U_2(\lambda, \phi) = \frac{1}{\sqrt{2}} \begin{pmatrix} 1 & -e^{i\phi} \\ e^{i\lambda} & e^{i(\lambda+\phi)} \end{pmatrix}$$
$$U_3(\lambda, \phi, \gamma) = \begin{pmatrix} \cos(\gamma/2) & -e^{i\lambda}\sin(\gamma/2) \\ -e^{i\phi}\sin(\gamma/2) & e^{i(\phi+\lambda)}\cos(\gamma/2) \end{pmatrix} \tag{3}$$

where for example, $U_1(\pi/4) = U_3(\pi/4, 0, 0) = T$, $U_1(\pi/2) = S$, $U_2(0, \pi) = H$. Hence, the Clifford+T gate set can be $\{U_1(\pi/2), U_2(0, \pi)$, CNOT, $U_1(\pi/4)\}$, and a hardware-specific native gate set is $\{U_1(\lambda), U_2(\lambda, \phi), U_3(\lambda, \phi, \gamma)$, CNOT$\}$.

We have chosen the PQC models in Figs. 6–9 as benchmark QML models identical to conventional benchmark deep learning (DL) models, such as Resnet [67]. The quantum resource required for executing them on the quantum machine is $\mathcal{O}(1)$ (constant time) if there is either no sign of T-gates or a low number of T-gates. In particular, we will deploy them on either the HPC system or the quantum machines depending on the existence and the number of T-gates in their configuration during the training phase. Furthermore, the number of T-gates defines the quantum resource required for deploying QML models on quantum computers.

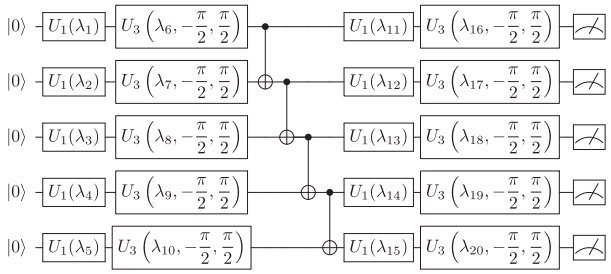

FIGURE 9. We transpiled a hardware-efficient quantum circuit having depth-one into the Clifford+T and the native gate set. This PQC is used for quantum variational inference by Benedetti et al. [74].

We used the symmetry-breaking concept inherited from conventional neural networks to determine the number of T-gates in our four PQCs [69]. Again, we strongly emphasize that QML models break the symmetry in their weights to decrease their redundant parameterized quantum gates, resulting in better generalization on unseen data points than conventional neural networks [18]. Namely, each weight within a parameterized quantum layer must have different digital values for capturing unique features. Therefore, we assumed that each layer of the QML models must have, at most, a single T-gate at each learning iteration, and our QML models having depth-one can only have one T-gate.

As for the quantum resource required for executing them on the quantum hardware, we assumed also the following.

1) If our PQCs have 10^8 T-gates and five logical qubits then we need 158 431 physical qubits (i.e., 9375 state distillation qubits, and 149 056 physical qubits) with a surface code distance of $d = 25$, and our QML models then take around 5 h per shot.
2) If our PQCs have three T-gates and five logical qubits then we need 50 700 physical qubits (i.e., 14 400 state distillation qubits, and 36 300 physical qubits) with a surface code distance of $d = 11$, and our QML models then take around 8.12^{-8} h per shot.
3) If our PQCs have one T-gate and five logical qubits, then we need 15 135 physical qubits (i.e. 14 400 state distillation qubits, and 735 physical qubits) with a surface code distance of $d = 7$, and our QML models then take around 2.07^{-8} h per shot.

Based on the study of the authors in [70] and [71], we estimated the quantum resources required for deploying QML models on error-correcting quantum machines known as surface code quantum computers. Our estimation considers that the quantum gate error is about $p = 10^{-3}$, and the single round of the surface code takes around 10^{-6} s. Here, the hours refer to T-gates preparation; Fowler and Gidney [70] provided a detailed spreadsheet for the quantum resource estimation. The quantum resource estimation demonstrates whether the QML models have to be deployed on quantum computers or not [64], [72], and it also generates the number of physical qubits required for deploying quantum algorithms on the surface code quantum computers.

III. CONCLUSION

We assessed the quantum resource required to execute QML models on a digital quantum computer to obtain a quantum advantage. We demonstrated that some quantum advantage can only be obtained if and only if QML models have a sufficient number of T-gates and generalize better on unseen data points than their classical counterparts. To count the T-gates of a particular QML model, we used the strong assumption that the QML models must break the symmetry in their weights—identical to the symmetry-breaking in conventional deep learning models—so that they become a more powerful model than their counterpart classical learning models. Based on the number of T-gates, we proposed a new HPC+QC paradigm (novel heterogeneous computing). In particular, we can simulate QML models on an HPC system (i.e., CPU+GPU) if they comprise a few hundred T-gates.

Toward quantum advantage in EO, we focused on QML models for hyperspectral images acquired by the EnMAP satellite since QML models can be trained on a limited labeled dataset, and our hyperspectral images have limited label information compared with multispectral images. For QML models, we utilized four parameterized quantum circuits and estimated the quantum resources required for deploying them on digital quantum machines. We found that we can deploy our QML models on an HPC system instead of a QC system since they only have a single T-gate due to the symmetry-breaking assumption. To design QML models with around $\mathcal{O}(10^8)$ that cannot be executed on an HPC system, they must have almost a depth of $\mathcal{O}(10^8)$, which is impractical for current and future quantum computers. Toward quantum advantage, it seems, therefore, reasonable to build, first, a special-purpose digital quantum computer for some practically significant computational task instead of a universal digital quantum computer similar to a D-Wave quantum annealer.

As future and ongoing work, we will invent and design a QML model with a reasonable depth that cannot be simulated on HPC systems but can be executed efficiently on QC systems and simultaneously has more expressive power over classical learning models.

ACKNOWLEDGMENT

The authors would like to thank the Gottfried Schwarz for reading, commenting, and improving the quality of this paper. This article is also part of the exploratory study dubbed "Quantum Advantage for Earth Observation (QA4EO)" granted by the European Space Agency.

REFERENCES

[1] M. Reichstein et al., "Deep learning and process understanding for data-driven Earth system science," *Nature*, vol. 566, no. 7743, pp. 195–204, Feb. 2019, doi: 10.1038/s41586-019-0912-1.

[2] P. Ebel, Y. Xu, M. Schmitt, and X. X. Zhu, "SEN12MS-CR-TS: A remote-sensing data set for multimodal multitemporal cloud removal," *IEEE Trans. Geosci. Remote Sens.*, vol. 60, 2022, Art. no. 5222414, doi: 10.1109/TGRS.2022.3146246.

[3] Y. Shi, X. X. Zhu, and R. Bamler, "Nonlocal compressive sensing-based SAR tomography," *IEEE Trans. Geosci. Remote Sens.*, vol. 57, no. 5, pp. 3015–3024, May 2019, doi: 10.1109/TGRS.2018.2879382.

[4] X. X. Zhu et al., "Deep learning meets SAR: Concepts, models, pitfalls, and perspectives," *IEEE Geosci. Remote Sens. Mag.*, vol. 9, no. 4, pp. 143–172, Dec. 2021, doi: 10.1109/MGRS.2020.3046356.

[5] G. Camps-Valls, J. Verrelst, J. Munoz-Mari, V. Laparra, F. Mateo-Jimenez, and J. Gomez-Dans, "A survey on Gaussian processes for Earth-observation data analysis: A comprehensive investigation," *IEEE Geosci. Remote Sens. Mag.*, vol. 4, no. 2, pp. 58–78, Jun. 2016, doi: 10.1109/MGRS.2015.2510084.

[6] D. Narmandakh, C. Butscher, F. D. Ardejani, H. Yang, T. Nagel, and R. Taherdangkoo, "The use of feed-forward and cascade-forward neural networks to determine swelling potential of clayey soils," *Comput. Geotechnics*, vol. 157, 2023, Art. no. 105319, doi: 10.1016/j.compgeo.2023.105319.

[7] A. Stritih, P. Bebi, and A. Grêt-Regamey, "Quantifying uncertainties in Earth observation-based ecosystem service assessments," *Environ. Model. Softw.*, vol. 111, pp. 300–310, 2019, doi: 10.1016/j.envsoft.2018.09.005.

[8] J. Pathak et al., "FourCastNet: A global data-driven high-resolution weather model using adaptive fourier neural operators," 2022, doi: 10.48550/arXiv.2202.11214.

[9] G. Cheng, X. Xie, J. Han, L. Guo, and G. S. Xia, "Remote sensing image scene classification meets deep learning: Challenges, methods, benchmarks, and opportunities," *IEEE J. Sel. Topics Appl. Earth Observ. Remote Sens.*, vol. 13, pp. 3735–3756, 2020, doi: 10.1109/JSTARS.2020.3005403.

[10] S. Arora and B. Barak, *Computational Complexity: A Modern Approach*. Cambridge, U.K.: Cambridge Univ. Press, 2009. [Online]. Available: https://www.cambridge.org/us/catalogue/catalogue.asp?isbn=9780521424264

[11] E. Farhi, J. Goldstone, S. Gutmann, and M. Sipser, "Quantum computation by adiabatic evolution," 2000, doi: 10.48550/arXiv.quant-ph/0001106.

[12] A. Lucas, "Ising formulations of many NP problems," *Front. Phys.*, vol. 2, 2014, doi: 10.3389/fphy.2014.00005.

[13] P. Rebentrost, M. Mohseni, and S. Lloyd, "Quantum support vector machine for Big Data classification," *Phys. Rev. Lett.*, vol. 113, Sep. 2014, Art. no. 130503, doi: 10.1103/PhysRevLett.113.130503.

[14] J. Allcock, C.-Y. Hsieh, I. Kerenidis, and S. Zhang, "Quantum algorithms for feedforward neural networks," *ACM Trans. Quantum Comput.*, vol. 1, no. 1, pp. 1–24, Oct. 2020, doi: 10.1145/3411466.

[15] J. Biamonte, P. Wittek, N. Pancotti, P. Rebentrost, N. Wiebe, and S. Lloyd, "Quantum machine learning," *Nature*, vol. 549, no. 7671, pp. 195–202, Sep. 2017, doi: 10.1038/nature23474.

[16] A. Abbas, D. Sutter, C. Zoufal, A. Lucchi, A. Figalli, and S. Woerner, "The power of quantum neural networks," *Nature Comput. Sci.*, vol. 1, no. 6, pp. 403–409, Jun. 2021, doi: 10.1038/s43588-021-00084-1.

[17] C. Gyurik and V. Dunjko, "On establishing learning separations between classical and quantum machine learning with classical data," Aug. 2023, doi: 10.48550/arXiv.2208.06339.

[18] T. Haug, K. Bharti, and M. Kim, "Capacity and quantum geometry of parametrized quantum circuits," *PRX Quantum*, vol. 2, Oct. 2021, Art. no. 040309, doi: 10.1103/PRXQuantum.2.040309.

[19] A. M. Childs, J.-P. Liu, and A. Ostrander, "High-precision quantum algorithms for partial differential equations," *Quantum*, vol. 5, Nov. 2021, Art. no. 574, doi: 10.22331/q-2021-11-10-574.

[20] A. J. Pool, A. D. Somoza, M. Lubasch, and B. Horstmann, "Solving partial differential equations using a quantum computer," in *Proc. IEEE Int. Conf. Quantum Comput. Eng.*, 2022, pp. 864–866, doi: 10.1109/QCE53715.2022.00146.

[21] N. Gourianov et al., "A quantum-inspired approach to exploit turbulence structures," *Nature Comput. Sci.*, vol. 2, no. 1, pp. 30–37, 2022, doi: 10.1038/s43588-021-00181-1.

[22] D-Wave Systems, "D-wave quantum computing," 2023, Accessed: Nov., 2023, doi: 10.1038/s43588-021-00181-1.

[23] C. Gross and I. Bloch, "Quantum simulations with ultracold atoms in optical lattices," *Science*, vol. 357, no. 6355, pp. 995–1001, 2017, doi: 10.1126/science.aal3837.

[24] L. Funcke, T. Hartung, K. Jansen, and S. Kühn, "Review on quantum computing for lattice field theory," in *Proc. 39th Int. Symp. Lattice Field Theory*, 2023, Art. no. 228. [Online]. Available: https://pos.sissa.it/430/228/pdf

[25] IBM, "IBM quantum computing," 2023. [Online]. Available: https://www.ibm.com/quantum

[26] A. Acín et al., "The quantum technologies roadmap: A European community view," *New J. Phys.*, vol. 20, no. 8, Aug. 2018, Art. no. 080201, doi: 10.1088/1367-2630/aad1ea.

[27] S. Aaronson, "How much structure is needed for huge quantum speedups?," 2022, doi: 10.48550/arXiv.2209.06930.

[28] M. Dalmonte, B. Vermersch, and P. Zoller, "Quantum simulation and spectroscopy of entanglement Hamiltonians," *Nature Phys.*, vol. 14, no. 8, pp. 827–831, Aug. 2018, doi: 10.1038/s41567-018-0151-7.

[29] S. Lu, M. C. Bañuls, and J. I. Cirac, "Algorithms for quantum simulation at finite energies," *PRX Quantum*, vol. 2, May 2021, Art. no. 020321, doi: 10.1103/PRXQuantum.2.020321.

[30] S. Otgonbaatar et al., "Quantum computing for climate change detection, climate modeling, and climate digital twin," Tech. Rep., Nov. 2023. [Online]. Available: https://elib.dlr.de/198760/

[31] R. Babbush, J. R. McClean, M. Newman, C. Gidney, S. Boixo, and H. Neven, "Focus beyond quadratic speedups for error-corrected quantum advantage," *PRX Quantum*, vol. 2, no. 1, Mar. 2021, Art. no. 010103, doi: 10.1103/prxquantum.2.010103.

[32] M. A. Nielsen, I. Chuang, and L. K. Grover, "Quantum computation and quantum information," *Amer. J. Phys.*, vol. 70, no. 5, pp. 558–559, 2002, doi: 10.1119/1.1463744.

[33] S. Otgonbaatar and M. Datcu, "Assembly of a coreset of Earth observation images on a small quantum computer," *Electronics*, vol. 10, no. 20, 2021, Art. no. 2482. [Online]. Available: https://www.mdpi.com/2079-9292/10/20/2482

[34] P. Helber, B. Bischke, A. Dengel, and D. Borth, "EuroSAT: A novel dataset and deep learning benchmark for land use and land cover classification," *IEEE J. Sel. Topics Appl. Earth Observ. Remote Sens.*, vol. 12, no. 7, pp. 2217–2226, Jul. 2019, doi: 10.1109/JSTARS.2019.2918242.

[35] R. Acharya et al., "Suppressing quantum errors by scaling a surface code logical qubit," *Nature*, vol. 614, no. 7949, pp. 676–681, Feb. 2023, doi: 10.1038/s41586-022-05434-1.

[36] S. Otgonbaatar and M. Datcu, "Classification of remote sensing images with parameterized quantum gates," *IEEE Geosci. Remote Sens. Lett.*, vol. 19, 2022, Art. no. 8020105, doi: 10.1109/LGRS.2021.3108014.

[37] P. Gawron and S. Lewiński, "Multi-spectral image classification with quantum neural network," in *Proc. IEEE Int. Geosci. Remote Sens. Symp.*, 2020, pp. 3513–3516, doi: 10.1109/IGARSS39084.2020.9323065.

[38] Y. Yang and S. Newsam, "Bag-of-visual-words and spatial extensions for land-use classification," in *Proc. 18th SIGSPATIAL Int. Conf. Adv. Geographic Inf. Syst.*, 2010, pp. 270–279, doi: 10.1145/1869790.1869829.

[39] S. Otgonbaatar, G. Schwarz, M. Datcu, and D. Kranzlmüller, "Quantum transfer learning for real-world, small, and high-dimensional remotely sensed datasets," *IEEE J. Sel. Topics Appl. Earth Observ. Remote Sens.*, vol. 16, pp. 9223–9230, 2023, doi: 10.1109/JSTARS.2023.3316306.

[40] S. Otgonbaatar and M. Datcu, "Natural embedding of the stokes parameters of polarimetric synthetic aperture radar images in a gate-based quantum computer," *IEEE Trans. Geosci. Remote Sens.*, vol. 60, 2022, Art. no. 4704008, doi: 10.1109/TGRS.2021.3110056.

[41] H.-Y. Huang et al., "Power of data in quantum machine learning," *Nature Commun.*, vol. 12, no. 1, May 2021, Art. no. 2631, doi: 10.1038/s41467-021-22539-9.

[42] M. K. Gupta, M. Beseda, and P. Gawron, "How quantum computing-friendly multispectral data can be?," in *Proc. Int. Geosci. Remote Sens. Symp.*, 2022, pp. 4153–4156, doi: 10.1109/IGARSS46834.2022.9883676.

[43] E. Boyda, S. Basu, S. Ganguly, A. Michaelis, S. Mukhopadhyay, and R. R. Nemani, "Deploying a quantum annealing processor to detect tree cover in aerial imagery of California," *PLoS One*, vol. 12, no. 2, pp. 1–22, 2017, doi: 10.1371/journal.pone.0172505.

[44] S. Otgonbaatar and M. Datcu, "Quantum annealing approach: Feature extraction and segmentation of synthetic aperture radar image," in *Proc. IEEE Int. Geosci. Remote Sens. Symp.*, 2020, pp. 3692–3695, doi: 10.1109/IGARSS39084.2020.9323504.

[45] D. Willsch, M. Willsch, H. De Raedt, and K. Michielsen, "Support vector machines on the D-wave quantum annealer," *Comput. Phys. Commun.*, vol. 248, 2020, Art. no. 107006, doi: 10.1016/j.cpc.2019.107006.

[46] G. Cavallaro, M. Riedel, M. Richerzhagen, J. A. Benediktsson, and A. Plaza, "On understanding Big Data impacts in remotely sensed image classification using support vector machine methods," *IEEE J. Sel. Topics Appl. Earth Observ. Remote Sens.*, vol. 8, no. 10, pp. 4634–4646, Oct. 2015, doi: 10.1109/JSTARS.2015.2458855.

[47] S. Otgonbaatar, M. Datcu, and B. Demir, "Coreset of hyperspectral images on a small quantum computer," in *Proc. IEEE Int. Geosci. Remote Sens. Symp.*, 2022, pp. 4923–4926, doi: 10.1109/IGARSS46834.2022.9884273.

[48] S. Otgonbaatar and M. Datcu, "A quantum annealer for subset feature selection and the classification of hyperspectral images," *IEEE J. Sel. Topics Appl. Earth Observ. Remote Sens.*, vol. 14, pp. 7057–7065, 2021, doi: 10.1109/JSTARS.2021.3095377.

[49] J. Chen, E. Stoudenmire, and S. R. White, "Quantum fourier transform has small entanglement," *PRX Quantum*, vol. 4, Oct. 2023, Art. no. 040318, doi: 10.1103/PRXQuantum.4.040318.

[50] E. M. Stoudenmire and D. J. Schwab, "Supervised learning with quantum-inspired tensor networks," 2016, Accessed: Nov., 2023, doi: 10.48550/arXiv.1605.05775.

[51] Z.-F. Gao et al., "Compressing deep neural networks by matrix product operators," *Phys. Rev. Res.*, vol. 2, Jun. 2020, Art. no. 023300, doi: 10.1103/PhysRevResearch.2.023300.

[52] F. Verstraete, T. Nishino, U. Schollwöck, M. C. Bañuls, G. K. Chan, and M. E. Stoudenmire, "Density matrix renormalization group, 30 years on," *Nature Rev. Phys.*, vol. 5, pp. 273–276, Apr. 2023, doi: 10.1038/s42254-023-00572-5.

[53] H. Huang, X.-Y. Liu, W. Tong, T. Zhang, A. Walid, and X. Wang, "High performance hierarchical tucker tensor learning using GPU tensor cores," *IEEE Trans. Comput.*, vol. 72, no. 2, pp. 452–465, Feb. 2023, doi: 10.1109/TC.2022.3172895.

[54] S. Otgonbaatar and D. Kranzlmüller, "Quantum-inspired tensor network for Earth science," in *Proc. IEEE Int. Geosci. Remote Sens. Symp.*, 2023, pp. 788–791, doi: 10.1109/IGARSS52108.2023.10282577.

[55] F. Fan, Y. Shi, T. Guggemos, and X. X. Zhu, "Hybrid quantum-classical convolutional neural network model for image classification," *IEEE Trans. Neural Netw. Learn. Syst.*, early access, Sep. 18, 2023, doi: 10.1109/TNNLS.2023.3312170.

[56] M. C. Caro et al., "Generalization in quantum machine learning from few training data," *Nature Commun.*, vol. 13, no. 1, Aug. 2022, Art. no. 4919, doi: 10.1038/s41467-022-32550-3.

[57] J. Preskill, "Quantum computing in the NISQ era and beyond," *Quantum*, vol. 2, 2018, Art. no. 79, doi: 10.22331/q-2018-08-06-79.

[58] S. Bravyi and D. Gosset, "Improved classical simulation of quantum circuits dominated by clifford gates," *Phys. Rev. Lett.*, vol. 116, Jun. 2016, Art. no. 250501, doi: 10.1103/PhysRevLett.116.250501.

[59] S. Aaronson and D. Gottesman, "Improved simulation of stabilizer circuits," *PhysRevA*, vol. 70, no. 5, Nov. 2004, doi: 10.1103/PhysRevA.70.052328.

[60] J. Tindall, M. Fishman, M. Stoudenmire, and D. Sels, "Efficient tensor network simulation of IBM's kicked Ising experiment," 2023, doi: 10.48550/arXiv.2306.14887.

[61] D. Litinski, "A game of surface codes: Large-scale quantum computing with lattice surgery," *Quantum*, vol. 3, Mar. 2019, Art. no. 128, doi: 10.22331/q-2019-03-05-128.

[62] M. Hinsche et al., "One T gate makes distribution learning hard," *Phys. Rev. Lett.*, vol. 130, Jun. 2023, Art. no. 240602, doi: 10.1103/PhysRevLett.130.240602.

[63] A. Mari, T. R. Bromley, J. Izaac, M. Schuld, and N. Killoran, "Transfer learning in hybrid classical-quantum neural networks," *Quantum*, vol. 4, Oct. 2020, Art. no. 340, doi: 10.22331/q-2020-10-09-340.

[64] M. E. Beverland et al., "Assessing requirements to scale to practical quantum advantage," 2022, doi: 10.48550/arXiv.2211.07629.

[65] G. Cheng, J. Han, and X. Lu, "Remote sensing image scene classification: Benchmark and state of the art," *Proc. IEEE*, vol. 105, no. 10, pp. 1865–1883, Oct. 2017, doi: 10.1109/JPROC.2017.2675998.

[66] M. Paoletti, J. Haut, J. Plaza, and A. Plaza, "Deep learning classifiers for hyperspectral imaging: A review," *ISPRS J. Photogrammetry Remote Sens.*, vol. 158, pp. 279–317, 2019, doi: 10.1016/j.isprsjprs.2019.09.006.

[67] K. He, X. Zhang, S. Ren, and J. Sun, "Deep residual learning for image recognition," 2015, doi: 10.48550/arXiv.1512.03385.

[68] E. Farhi and H. Neven, "Classification with quantum neural networks on near term processors," 2018, doi: 10.48550/arXiv.1802.06002.

[69] R. Fok, A. An, and X. Wang, "Spontaneous symmetry breaking in neural networks," 2017, doi: 10.48550/arXiv.1710.06096.

[70] A. G. Fowler and C. Gidney, "Low overhead quantum computation using lattice surgery," 2019, doi: 10.48550/arXiv.1808.06709.

[71] C. Gidney, "Stim: A fast stabilizer circuit simulator," *Quantum*, vol. 5, Jul. 2021, Art. no. 497, doi: 10.22331/Fq-2021-07-06-497.

[72] M. Reiher, N. Wiebe, K. M. Svore, D. Wecker, and M. Troyer, "Elucidating reaction mechanisms on quantum computers," *Proc. Nat. Acad. Sci.*, vol. 114, no. 29, pp. 7555–7560, 2017, doi: 10.1073/pnas.1619152114.

[73] M. Schuld, A. Bocharov, K. M. Svore, and N. Wiebe, "Circuit-centric quantum classifiers," *Phys. Rev. A*, vol. 101, no. 3, Mar. 2020, doi: 10.1103/PhysRevA.101.032308.

[74] M. Benedetti, B. Coyle, M. Fiorentini, M. Lubasch, and M. Rosenkranz, "Variational inference with a quantum computer," *Phys. Rev. Appl.*, vol. 16, Oct. 2021, Art. no. 044057, doi: 10.1103/PhysRevApplied.16.044057.